Sustainable Energy Technologies and Assessments 55 (2023) 102951

Contents lists available at ScienceDirect

Sustainable Energy Technologies and Assessments

journal homepage: www.elsevier.com/locate/seta

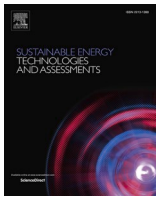

Green building's heat loss reduction analysis through two novel hybrid approaches

Hossein Moayedi [a,b,*], Hasan Yildizhan [c], Pasura Aungkulanon [d,*], Yulineth Cardenas Escorcia [e], Mohammed Al-Bahrani [f], Binh Nguyen Le [a,b]

[a] Institute of Research and Development, Duy Tan University, Da Nang, Viet Nam
[b] School of Engineering & Technology, Duy Tan University, Da Nang, Viet Nam
[c] Department of Energy Systems Engineering, Faculty of Engineering, Adana Alparslan Turkes Science and Technology University, Adana, 01250 Sarıçam, Turkey
[d] Faculty of Engineering, King Mongkut's University of Technology North Bangkok, Bangkok 10800, Thailand
[e] Research Group GIOPEN, Energy Department, Universidad de la Costa (CUC), Barranquilla 080016, Colombia
[f] Chemical Engineering and Petroleum Industries Department, Al-Mustaqbal University College, Babylon 51001, Iraq

ARTICLE INFO

Keywords:
Heat loss
Green building
Energy efficiency
Artificial intelligence

ABSTRACT

One of the key reasons for the performance discrepancy between a building's intended usage and the actual operation is Heat Loss, which describes a building's envelope efficiency during in-use circumstances. In this setting, the ANN models' use for energy analysis of green buildings has become more established. This research aims to anticipate the heat loss of green buildings utilizing two artificial neural network-based methodologies (ANN). In particular, TLBO and BBO are used and contrasted. Additionally, RMSE, MAE, and R2 are used to calculate an absolute error for predicting heat loss to gauge the accuracy of the findings. The suggested TLBO-MLP standard is a reliable method with a positive outcome (RMSE = 0.01012 and 0.05216, and R2 = 0.99536 and 0.9651). Also, according to the training error ranges of [−0.0006078, 0.01133] and [−0.00040708, 0.010181] and testing error ranges of [0.0004724, 0.068666] and [0.0021984, 0.057688] for BBO-MLP and TLBO-MLP, respectively, shows that the TLBO-MLP reaches the lower range of error and can predict the heat loss with higher accuracy and it could properly forecast the heat loss of building technologies. Even so, the BBO-MLP standard provides this research with satisfactory performance (R2 = 0.9943 and 0.95175, and RMSE = 0.01122 and 0.06112). To increase the precision of calculating the heat loss of buildings, specifically integrating them with optimization algorithms, further study is required.

Introduction

A new review by the Intergovernmental Panel on Climate Change [1] illustrated that the most significant increase in carbon emissions emanates from electricity generation, industry, transport, and building operations [2]. The building section allocates for almost 40 % of the whole energy utilization in various countries; this illustrates the significance of reducing energy utilization in mentioned industry [3–5].

In oil-rich and oil-producing nations, there is a pressing demand for rapid energy conservation because of dwindling supplies, restricted accessibility, and rising prices for energy everywhere in the world [6]. Increasing the thermal insulation of buildings is an essential factor in saving energy [7,8]. This is especially important in warm regions, where there is a relatively large requirement for energy to be used in chilling via air conditioning [9]. The thermal conductivity of the cell matrix and the cell walls, as well as convection and radiation, are major determinants of thermal properties, with the cell matrix playing the most significant role in determining the total thermal transmission features. Concerns regarding the environment and energy have captured the attention of people all across the world in recent years [10]. 30 % of the initial energy usage in the world and nearly-one-third of the world's carbon emissions are attributable to the construction industry [11]. Because of increased urbanization, climate change, future water resources, and other factors, global building energy demand has constantly been growing [10,12,13].

The pertinent criteria emphasize the enhancement of thermal function, and associated regulations are absent. Nevertheless, assuming only the thermal performance appears to be against the notion of green

* Corresponding authors at: Institute of Research and Development, Duy Tan University, Da Nang, Viet Nam (H. Moayedi).
E-mail addresses: hosseinmoayedi@duytan.edu.vn (H. Moayedi), pasura.a@eng.kmutnb.ac.th (P. Aungkulanon).

https://doi.org/10.1016/j.seta.2022.102951
Received 13 September 2022; Received in revised form 13 November 2022; Accepted 12 December 2022
Available online 26 December 2022

Table 1
Wall types with indoor, outdoor, and external surface temperature.

Wall types and heat transfer coefficients	Coating Material and heat transfer coefficients	Indoor Temperature (°C) (14:15–17:00)	Outdoor Temperature (°C) (14:15–17:00)	External Surface Temperature (°C) (14:15–17:00)
	XPS (0.035 W/mK)		−4.2–18.6	−0.3–19.6
Reinforced concrete (2.1 W/mK)	EPS (0.040 W/mK)	21–22.3		0–20
	Aerogel Insulation Plaster (0.013 W/mK)			−0.4–19.4
	Plaster (1 W/mK)			2.1–21
	XPS (0.035 W/mK)		−4.2–18.6	−0.6–19.2
	EPS (0.040 W/mK)	21–22.3		−0.5–19.7
Red Brick (0.45 W/mK)	Aerogel Insulation Plaster (0.013 W/mK)			−1.1–19
	Plaster (1 W/mK)			0.9–20.3
	XPS (0.035 W/mK)		−4.2–18.6	−1–19
	EPS (0.040 W/mK)	21–22.3		−0.9–19.6
Aerated Concrete (0.11 W/mK)	Aerogel Insulation Plaster (0.013 W/mK)			−2.1–18.8
	Plaster (1 W/mK)			0.3–20.2
	XPS (0.035 W/mK)		−4.2–18.6	−0.6–19.3
	EPS (0.040 W/mK)	21–22.3		−0.7–19.8
Briquette (0.63 W/mK)	Aerogel Insulation Plaster (0.013 W/mK)			−0.9–19.1
	Plaster (1 W/mK)			1.1–20.5

building. It is still necessary to research and examine whether an improvement in the building environment's thermal function can significantly save energy and environmental and economic advantages [3,8]. The exact building exterior structure has been optimized by several investigators using optimization selection methods and building simulation software with the goal of improving thermal performance, expense, and environmental effects [14–19]. Often, different techniques correlate to the building's thermal function as described in pertinent standards. Deployment of multi-index assessment methods can lead to building exterior designs' development. The actual thermal usage in operating conditions is influenced by a variety of parameters, including actual external temperature variations, people working habits, the matching of efficiency improvement between exterior structures, etc., even though the green building's thermal performance has been enhanced based on conventional constructions [9,20,21]. This causes a significant disparity between the factual thermal consumption and those calculated by modeling. There is typically a divergence between a compartment's actual and expected overall thermal performance.

With the expansion of the Green Building's Assessment Standard and building energy efficiency standards, the necessities for building envelope's thermal performances have gently improved [22,23]. However, just considering the thermal implementation versus the residential building's concept, the related standards pay much consideration to improve the thermal performance, and there is a deficiency of corresponding suggestions and regulations on selecting materials [24,25]. Various researchers have utilized software to simulate buildings and tools for optimization selection to optimize a particular building structure with the thermal implementation, environmental impact, and cost as targets [26–35].

In various engineering inquiries, ANNs are a subject of utmost significance [36]. Various thermal transmission applications have extensively used these networks, including predicting building heating loads, wasted heat retrieval, solar energy, heat exchangers, etc. [27,35,37–40]. The characteristics of a jet impingement nanofluid flow within a microchannel heat sink were anticipated by Naphon et al. [41] using artificial neural networks in conjunction with computational fluid dynamics. During the training phase, the Levenberg-Marquardt Backward propagation (LMB) was considered to optimize the error ratio and create the best possible ANN model. There was a proportion of 1.25 percent error between the outcomes that were determined and those that were predicted. Acikgoz et al. [16] conducted a series of experiments in an experimental chamber with unchanged dimensions to study the thermal transport's characteristics in a room of realistic size. Studying the thermal characteristics of radiant heating was accomplished using ANN methods [42]. In this instance, it was determined that the Levenberg-Marquardt approach was the most precise. An ANN was used by Moya-Rico [43] to forecast the thermal exchange and TTHE pressure drop. Corrugated and smooth inner tubes were subjected to empirical assessment, and a fluid employed in the food industry was a working fluid. They discovered that an ANN model containing two hidden layers provided an excellent agreement with the empirical data. The mean relative error was approximately 1.91 percent for the thermal transmission and 3.82 percent for the pressure drop.

Due to the increasing cost of energy and climate changes, it was necessary to decrease the use of carbon-based energy sources'. An effective measure that can be utilized in this regard is the building's thermal insulation [44]. Remaining energy used for heat insulation in buildings, CO2 emissions are decreased. An experimental study has been done in the current article. It took a year to collect the dataset. The collected dataset contains different wall materials. Then, the effect of different thermal insulation materials on CO2 emissions was studied experimentally, and the energy performance of different wall types was examined with different insulation materials and their effects on CO2 emissions were investigated (section 2, Table 1). Afterwards, artificial intelligence was used to predict the heat loss. For this purpose, first of all multi-layer perception was applied to the model. Results indicate that swarm intelligent methods can accurately predict the heat loss. Finally, two hybrid algorithms; namely BBO and TLBO, were used to evaluate the accuracy rate of predicting these methods in predicting the heat loss. But also, further studies are required to increase the precision of calculating the heat loss of buildings and explicitly integrating them with optimization algorithms.

To forecast the heat loss reduction analyses in thermal insulating materials, an ANN is used in this research. The ANN is associated with two nature-inspired optimization techniques [45]. The mathematical analyses allow collecting the data sets necessary for the ANN's training. The thermal transmission coefficients of the wall (W/mK), the thermal transmission coefficients of the coating material (W/mK), the outside and inside temperatures, and the external surface temperature are all taken into account when calculating the amount of heat loss reduction. Because of their high accuracy and wide applicability, the models established in this study can be used for various purposes, including performing heat loss reduction analyses on thermal insulating compounds.

This overview is divided into five sections. The datasets and

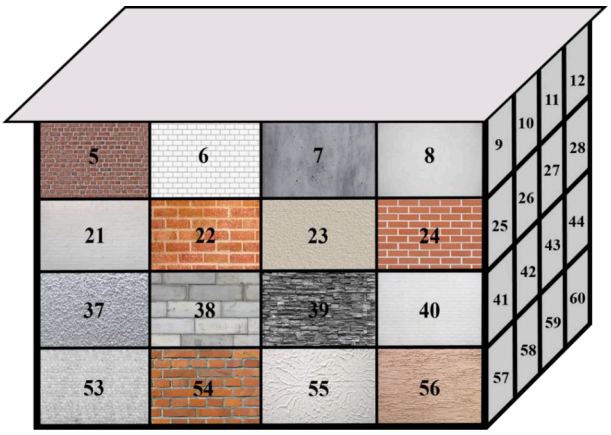

Fig. 1. A 3D view of different wall types.

attributes used in the heat loss prediction and the research data and predicting model are reviewed in section 2. Section 3 will cover the presentation of the methods and materials. The results are presented in Section 4, along with an explanation of the analysis and the conclusions obtained when the training and test datasets were built using ANN approaches. The paper has reached its conclusion, and section 5 summarizes the approaches used to decide which combinations are optimal.

Established database

Reducing reliance on carbon-based energy sources is necessary because of the converging factors of increasing energy expenses and climate change [5]. The installation of thermal insulation in buildings is one of the strategies that can be utilized in this context, which is among the most efficient of the available options. CO2 emissions can be lowered in buildings by using less energy for heating and cooling and heat insulation [26]. Experiments are carried out for this investigation to explore the effect of various thermal insulation applications on CO_2 emissions in the climatic situations of Hakkari. Using different insulating materials (plaster, eps, xps, aerogel) for this objective, the energy performance of several wall types (red brick, reinforced concrete, aerated concrete, and briquette) is tested as well as their impacts on CO_2 emissions (Fig. 1 and Table 1).

The thermal transmission coefficients of the wall (W/mK), the thermal transmission coefficients of the coating material (W/mK), the interior temperature, the exterior temperature, and the external surface temperature are the parameters that are used as inputs, and the amount of heat loss (W) is output variable in this study. Fig. 2 illustrates both the input and output layers of the distribution system (Table 2).

Methodology

Maps, modeling approaches, model validation, and optimization algorithm analysis are required to be used to perform the three tasks outlined before in this part successfully. Detailed explanations of each phase are provided below, and the flow chart of the current research is illustrated in Fig. 3.

Artificial neural network

In a virtual environment, simulations of the human nervous system like ANN seek to represent the organization and function of the nervous system of humans [46,47]. Employing a neural network containing artificial neural interconnections, it is feasible to get an estimate or approximation of a function [48,49]. Two input and output layers and hidden layers for feature manipulation are common components of an ANN [50]. Fig. 2 presents the ANN model used for this study. There has been a substantial expansion in the use of neural networks for forecasting and categorizing data in recent decades [51]. This network possesses at least one hidden layer in addition to having output and input. The data for this network is divided into two parts: training and testing. ANN is an aggregation of many perceptrons or neurons at each layer. Whenever input data is categorized in the forward orientation, this network is called a feed-forward neural network. The output, hidden, and input layers make up the fundamental layers of an ANN. The input layer receives the data, which is then processed by the hidden levels, and the outcomes are returned by the output layer [52]. Specific decimal weights that will be used after learning are learned by the layers comprising the neural network [53].

Images, text, and data tables respond favorably to the ANN approach. When dealing with nonlinear functions and learning weights, ANN possesses the benefit of being able to translate any input into an output efficiently [54]. This gives it a competitive advantage. A universal estimation is a complex connection between input and output data learned by an ANN since the activation functions are nonlinear. Within the realm of science, the application of ANNs is becoming an increasingly prevalent practice [55,56].

Fig. 3 is an illustration of the artificial neural network's underlying structure. The weights of all inputs are added together for each neuron output via activation functions, and the weights of all neuron inputs are added together for each bias weight. To obtain gradients, the neural network weights are updated with the help of backpropagation. During backward propagation, the gradient has a chance of completely disappearing or exploding [57].

Hybrid model development

The MLP is used in conjunction with two optimizer methods, the BBO and the TLBO, to achieve the greatest possible performance with the lowest possible error rate. Fig. 3 depicts the attributes and construction of the regarded ANN, which has five neurons in its hidden layer. This ANN is used to anticipate the heat loss (W) in contexts of the thermal transfer coefficients of the wall (W/mK), the thermal transfer coefficients of the coating material (W/mK), the inside temperature, the outside temperature, external surface temperature, and finally the output variable. It is essential to point out that to implement the ANN containing five neurons while maintaining the least amount of error possible, the trial-and-error technique is considered. By assigning biases and weights, these networks compute outputs. The network structure is theoretically added to the evolutionary processes to make the ANN as optimal as possible. The weights and biases of the unreinforced ANN are being replaced with the best possible alternatives using optimization methods in the present investigation. It is important to remember that the algorithms mentioned above are carried out among ten communities (i.e., 50, 100, 150, 200, 250, 300, 350, 400, 450, and 500). Calculating RMSE and R^2 to assess the suggested algorithms requires Eqs. (1) and (2), respectively.

$$RMSE = \sqrt{\frac{1}{N}\sum_{i=1}^{N}\left[\left(Y_{i_{simulated}} - Y_{i_{predicted}}\right)\right]^2} \tag{1}$$

$$R^2 = 1 - \frac{\sum_{i=1}^{N}\left(Y_{i_{simulated}} - Y_{i_{predicted}}\right)^2}{\sum_{i=1}^{N}\left(Y_{i_{simulated}} - \overline{Y}_{i_{simulated}}\right)^2}, \overline{Y}_{i_{simulated}} = \frac{1}{n}\sum_{i=1}^{N} Y_{i_{simulated}} \tag{2}$$

Biogeography–based optimization algorithm (BBO)

The scientific study of the patterns of the geographical dispersion of living things through space and time is known as biogeography [58]. In the early 19th century, Wallace and Darwin were the first researchers to research this subject. The numerical models of island biogeography developed by MacArthur and Wilson [59] in the 1960s demonstrate that the type abundance of the island might be anticipated in terms of characteristics like habitat region, extinction percentage, and

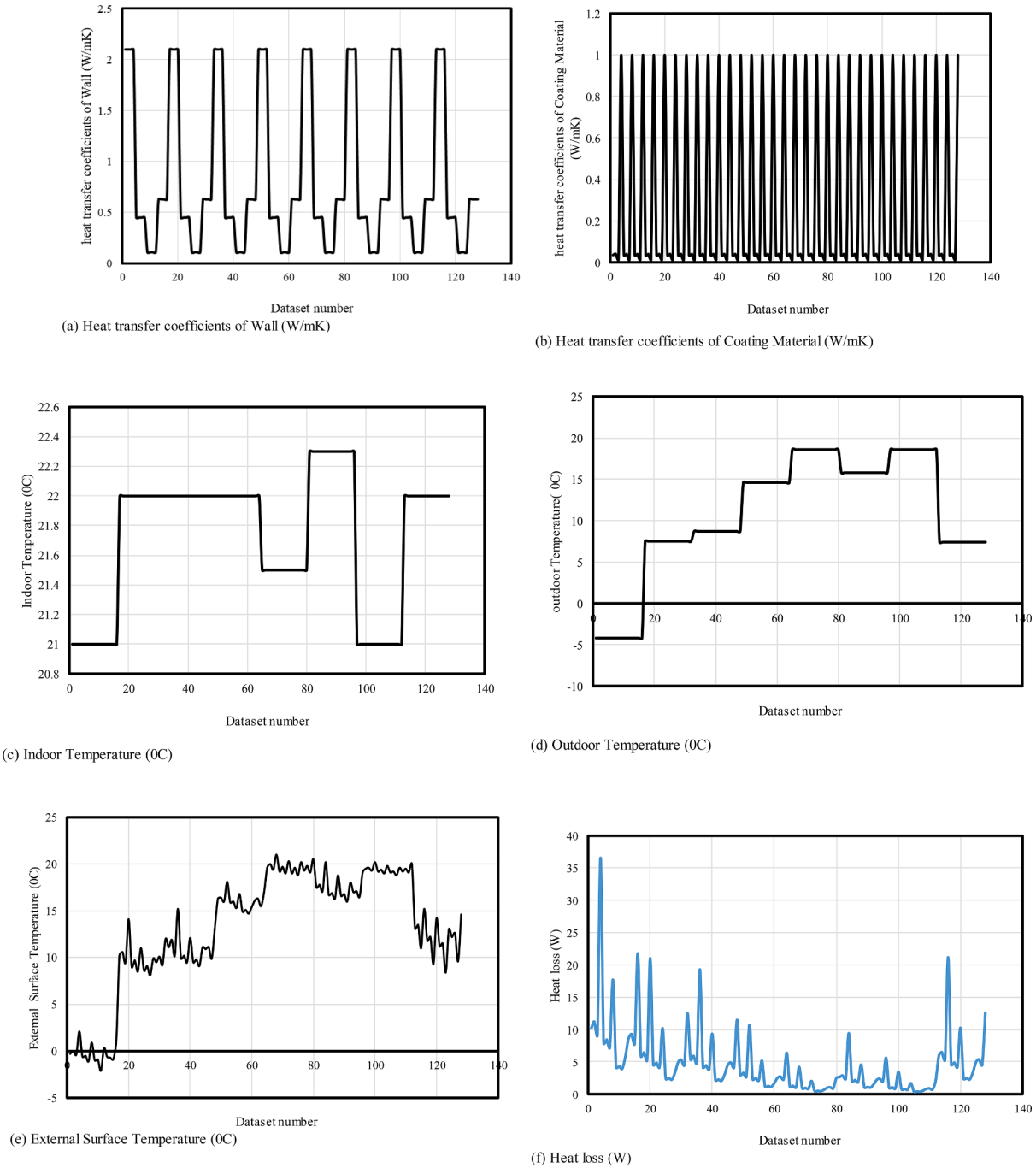

(a) Heat transfer coefficients of Wall (W/mK)

(b) Heat transfer coefficients of Coating Material (W/mK)

(c) Indoor Temperature (0C)

(d) Outdoor Temperature (0C)

(e) External Surface Temperature (0C)

(f) Heat loss (W)

Fig. 2. The graphically distribution of the input and output layers.

Table 2
Neural network optimization results.

Number of neurons	Network results			Scoring			Total score	RANK
	$RMSE_{total}$	$RMSE_{train}$	$RMSE_{test}$	$RMSE_{total}$	$RMSE_{train}$	$RMSE_{test}$		
1	0.515	0.481	0.505	2	2	2	6	9
2	0.495	0.456	0.484	3	3	3	9	8
3	0.367	0.372	0.369	5	6	6	17	5
4	0.271	0.302	0.281	8	8	8	24	3
5	0.570	0.550	0.564	1	1	1	3	10
6	0.126	0.155	0.135	10	10	10	30	**1**
7	0.238	0.294	0.256	9	9	9	27	2
8	0.490	0.452	0.479	4	4	4	12	7
9	0.359	0.397	0.371	6	5	5	16	6
10	0.330	0.305	0.322	7	7	7	21	4

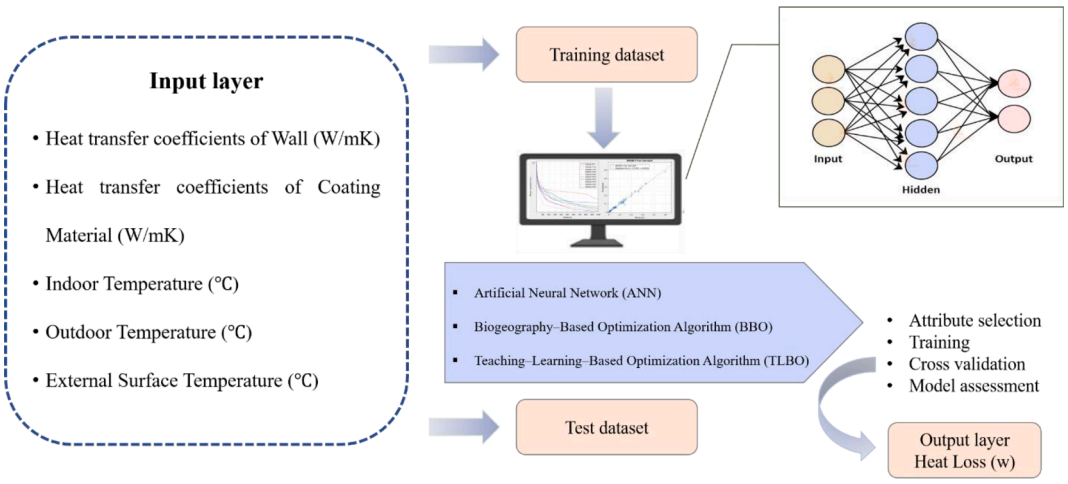

Fig. 3. (a) The flow chart of recent study. (b) The basic structure of MLP in the current study.

Table 3
Network results based on two statistical indices for various proposed BBOMLP swarm size.

Swarm size	Training dataset		Testing dataset		Scoring				Total Score	Rank
	RMSE	R^2	RMSE	R^2	Training		Testing			
50	0.01266	0.99273	0.06533	0.94467	6	6	9	9	30	2
100	0.01427	0.99075	0.06685	0.942	4	4	8	8	24	3
150	0.01199	0.99348	0.07738	0.92145	9	9	3	3	24	3
200	0.01496	0.98983	0.0677	0.94045	3	3	7	7	20	6
250	0.01418	0.99087	0.10254	0.8573	5	5	1	1	12	9
300	0.01223	0.99322	0.08521	0.90387	8	8	2	2	20	6
350	0.01262	0.99278	0.07451	0.92738	7	7	4	4	22	5
400	0.0174	0.98622	0.07289	0.93064	1	1	5	5	12	9
450	0.0159	0.98851	0.06894	0.93818	2	2	6	6	16	8
500	**0.01122**	**0.9943**	**0.06112**	**0.95175**	**10**	**10**	**10**	**10**	**40**	**1**

immigration rate. Simon [60] established the BBO algorithm by applying the island biogeography's mathematics to the problem. In this algorithm, a strategy is similar to an island, the elements of the solution are comparable to a collection of suitability index variables (SIVs), and the solution fitness is similar to the island's species richness or habitat suitability index (HSI). An essential part of the algorithm is the equilibrium hypothesis of island biogeography, suggesting that islands with a higher HSI possess a high level of species migration, and islands with a lower HSI experience a high rate of species migration. The straightforward linear species diversity's model in a single island is depicted in

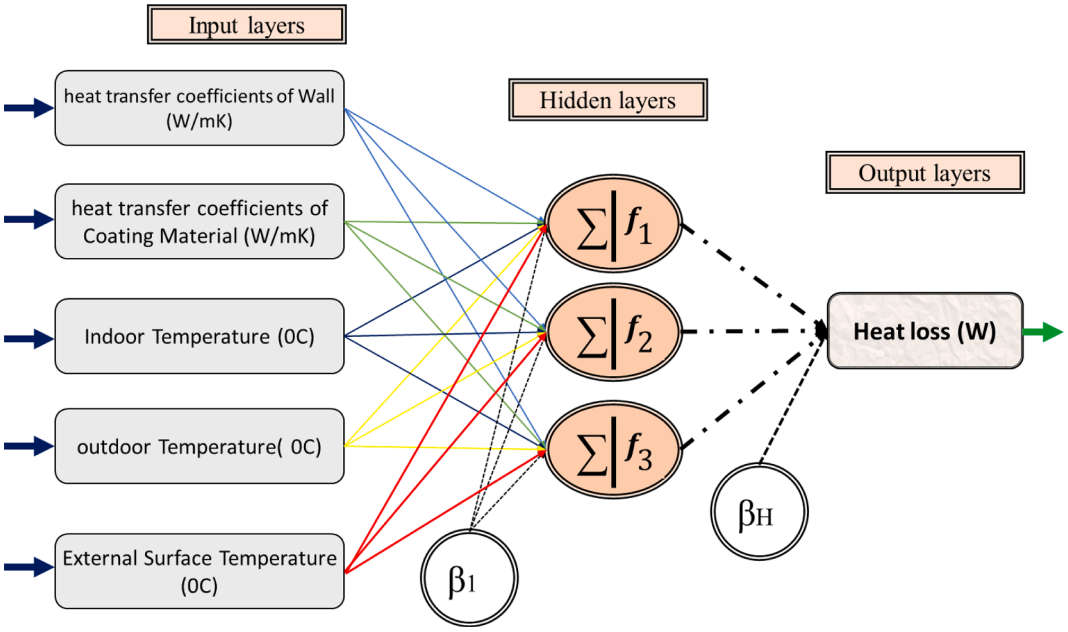

Fig. 4. The variation of the mean square error for the (a) bbomlp, and (b) tlbomlp predictive network.

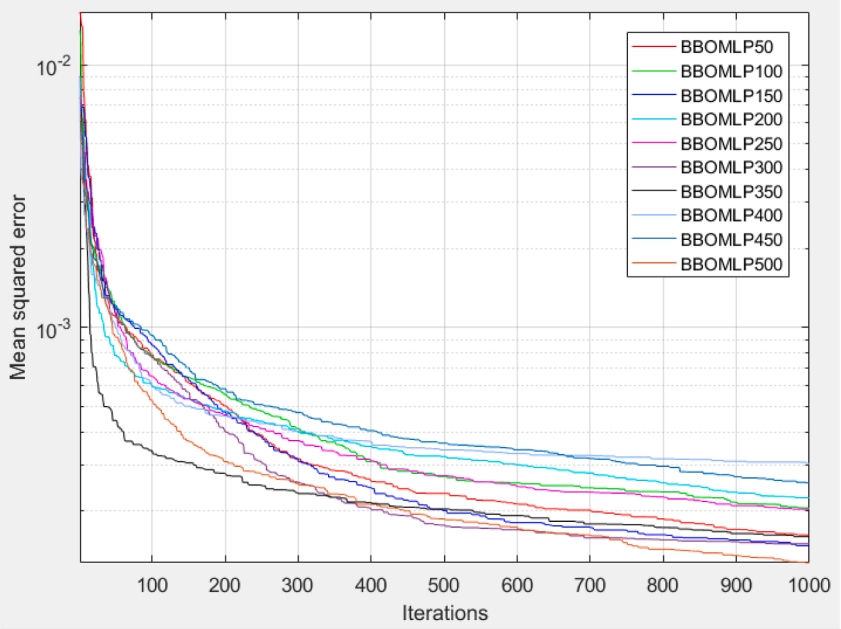

(a) BBOMLP

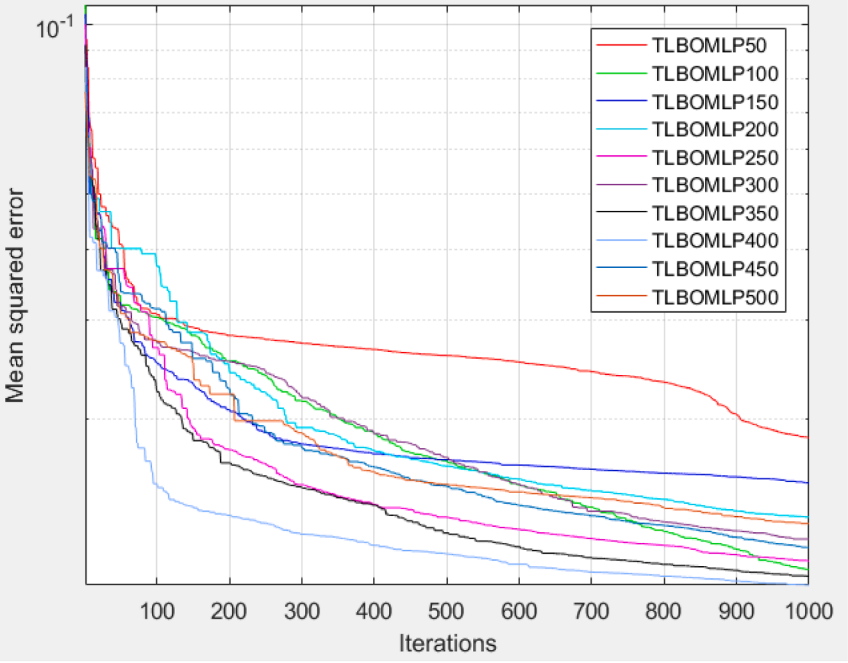

(b) TLBOMLP

Fig. 5. Accuracy results of training dataset for different proposed BBOMLP structure.

Fig. 1. According to this model, the rate of emigration μ and the rate of immigration λ are both functions of the island's HSI value [60,61].

Migration and mutation are the two types of operators employed by BBO. An SIV is moved from an emigrating island to another one that is immigrating at any time by the migration operator. These islands are chosen in a probabilistic manner according to the μ and λ rates. Based on the steady-state probability p of species number on the island, the mutation operator will randomly alters an SIV. Algorithm 1 indicates the fundamental BBO technique, where *rand*() produces a real number which is selected randomly in the range of [0,1] and $rand_d$() produces a random amount in the range of the dth SIV.

Algorithm 1. *A basic algorithm of BBO*

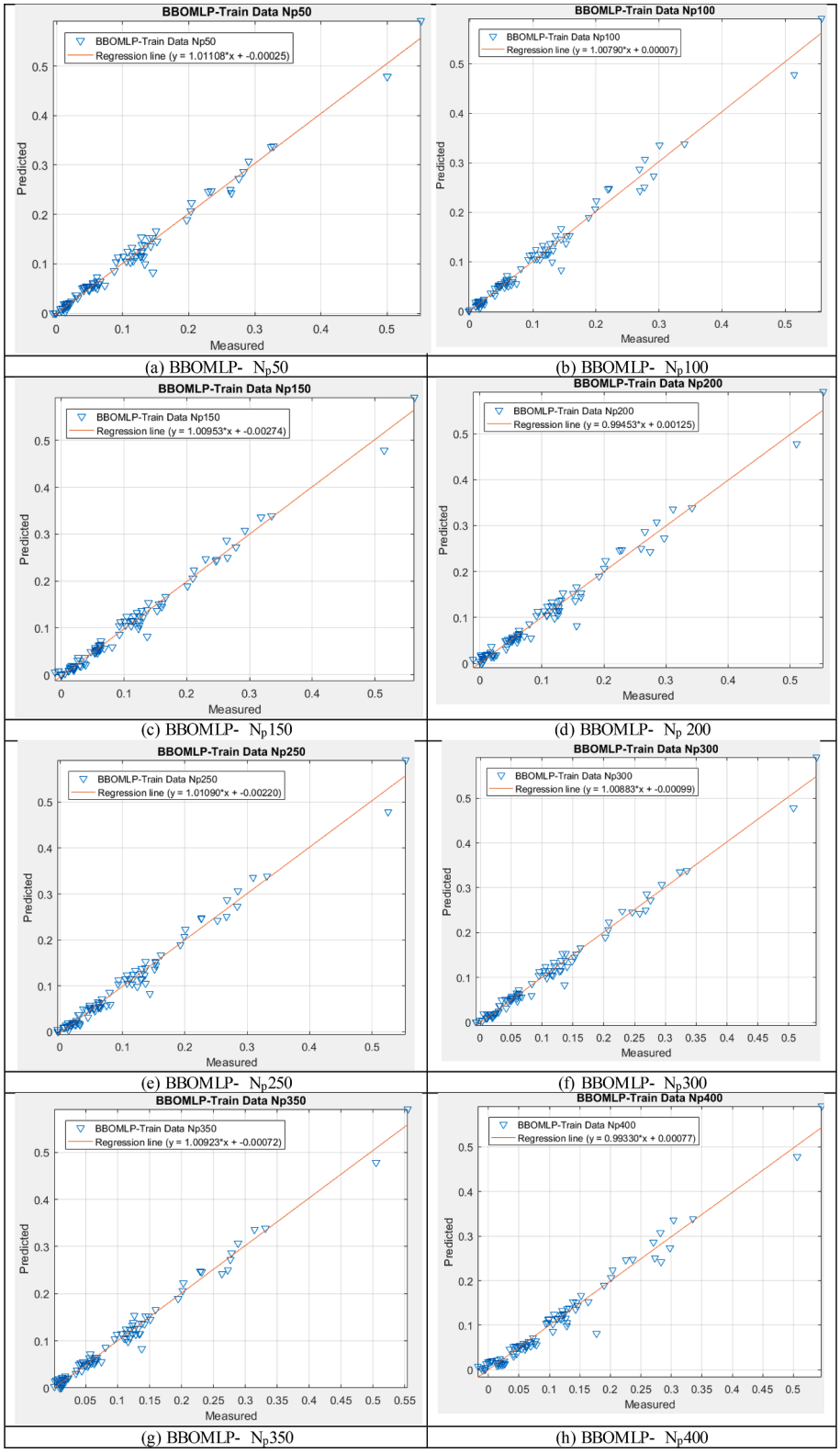

Fig. 6. Accuracy results of testing dataset for different proposed BBOMLP structure.

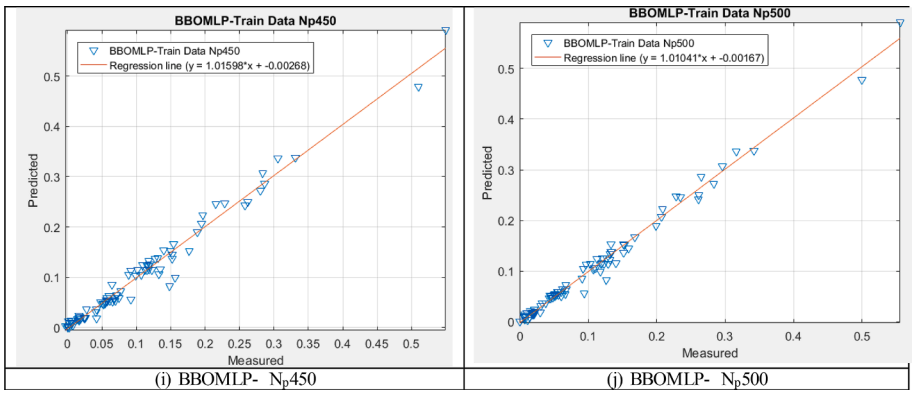

(i) BBOMLP- N_p450 (j) BBOMLP- N_p500

Fig. 6. (*continued*).

Table 4
Network results based on two statistical indices for various proposed TLBOMLP swarm size.

	Training dataset		Testing dataset		Scoring				Total Score	Rank
Swarm size	RMSE	R^2	RMSE	R^2	Training		Testing			
50	0.01849	0.98442	0.07228	0.93183	1	1	1	1	4	10
100	0.01078	0.99474	0.04257	0.97689	8	8	10	10	36	2
150	0.01537	0.98926	0.06725	0.94127	2	2	4	4	12	8
200	0.01337	0.99188	0.07115	0.93402	3	3	2	2	10	9
250	0.01115	0.99436	0.05968	0.95405	7	7	6	6	26	4
300	0.01222	0.99322	0.06053	0.9527	5	5	5	5	20	6
350	0.01049	0.99502	0.05534	0.96062	9	9	8	8	34	3
400	**0.01012**	**0.99536**	**0.05216**	**0.9651**	**10**	**10**	**9**	**9**	**38**	**1**
450	0.01181	0.99368	0.05965	0.95411	6	6	7	7	26	4
500	0.013	0.99233	0.06774	0.94039	4	4	3	3	14	7

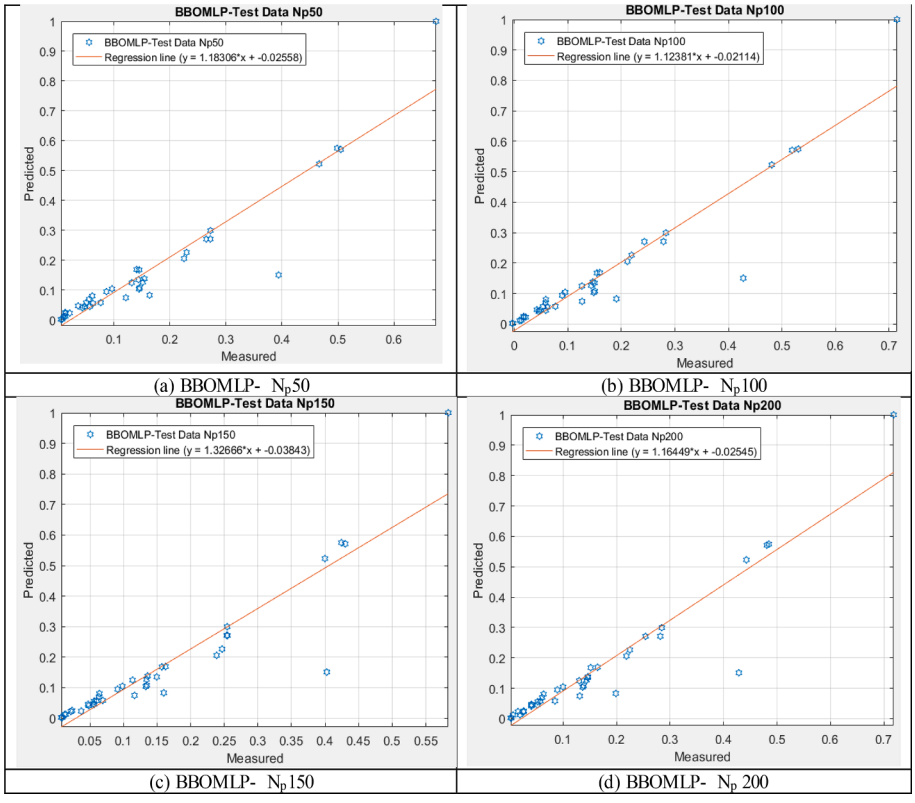

(a) BBOMLP- N_p50 (b) BBOMLP- N_p100

(c) BBOMLP- N_p150 (d) BBOMLP- N_p 200

Fig. 7. Accuracy results of training dataset for different proposed TLBOMLP structure.

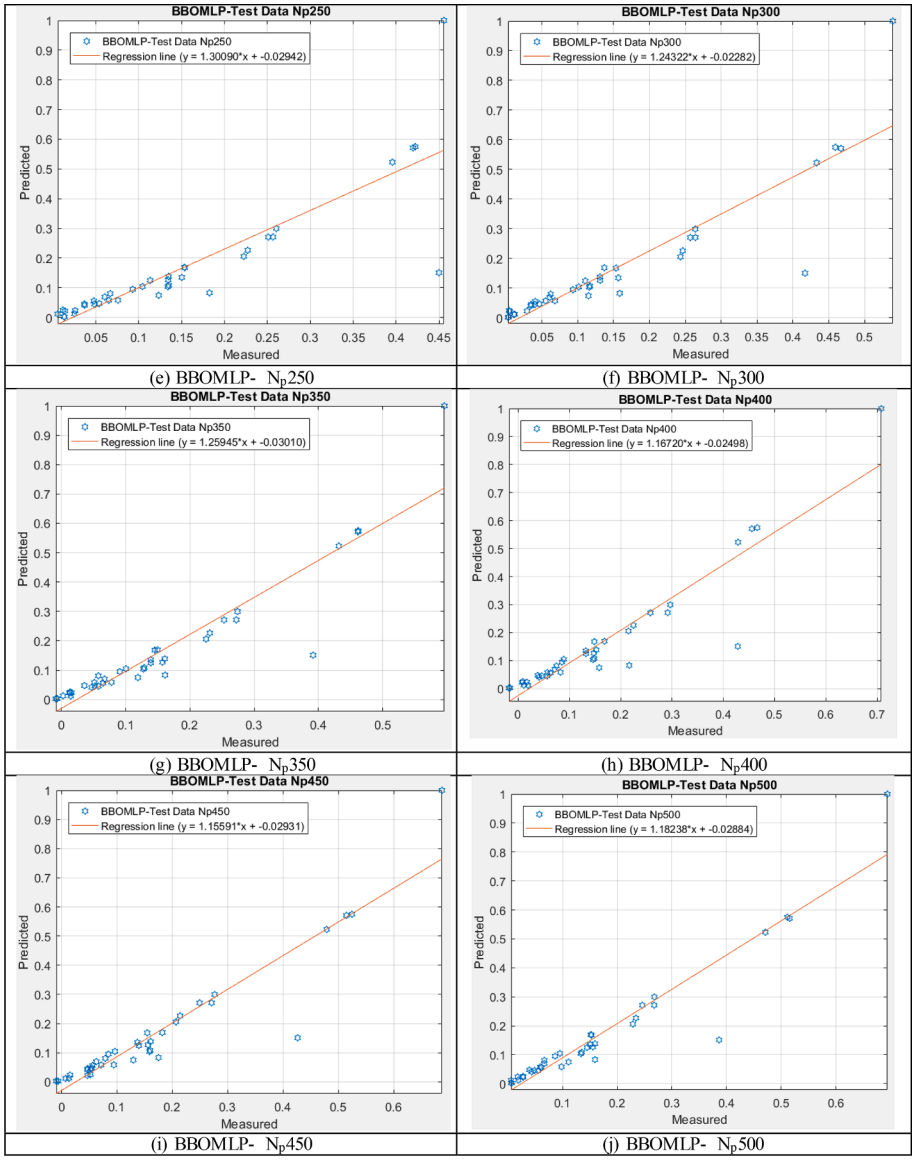

Fig. 7. (*continued*).

```
1  Randomly initialize a population P of n islands (solutions) to the problem;
2  while stop criterion is not satisfied do
3    Calculate λ_i, μ_i, and p_i for each island X_i;
4    for each X_i ∈ P do
5      for each SIV X_{i,d} of the island do
6        if rand() < λ_i then
7          Select an emigrating island X_j with probability ∝ μ_j;
8          X_{i,d} ← X_{j,d}; //migration
9    for each X_i ∈ P do
10     for each SIV X_{i,d} of the island do
11       if rand() < p_i then
12         X_{i,d} ← rand_d(); //mutation
13   Evaluate the fitness values of the habitats;
14 return the best known solution.
```

It is important to note that, in the most recent version of the BBO code, which was published by Simon [60], it is recommended to carry out one more iteration of fitness analysis and sort the solution before each generation's mutations. The algorithm's effectiveness may be improved by this implementation; nevertheless, this increases the frequency of function evaluations (NFE) performed during each generation. Our new approach can significantly enhance performance with only n function assessments per generation, as will be observed in the following section assuming a population size of n. The direct cloning of an SIV from one island to another, conducted by the primary BBO's migration operator, restricts the component variety of emerging islands. Ma and Simon [31] established the mixed BBO (B-BBO), and it takes advantage of the mixed migration to substitute Line 8 of Algorithm 1, as seen in the following:

$$X_{i,d} = \alpha X_{i,d} + (1-\alpha)X_{j,d} \tag{3}$$

where α indicates a real number between 0 and 1. Although it was suggested for limited optimization in Ref. [62], the B-BBO technique works better than the basic BBO on various other optimization issues.

Teaching–Learning–Based optimization algorithm (TLBO)

Every person should make an effort to improve himself by picking up new skills from the experiences of others as part of an essential process (teaching–learning) [24]. TLBO is the name of an algorithm that was developed by Rao et al. [63,64] and Rao and Patel [65]. This algorithm imitates the classic teaching and learning process in a classroom setting

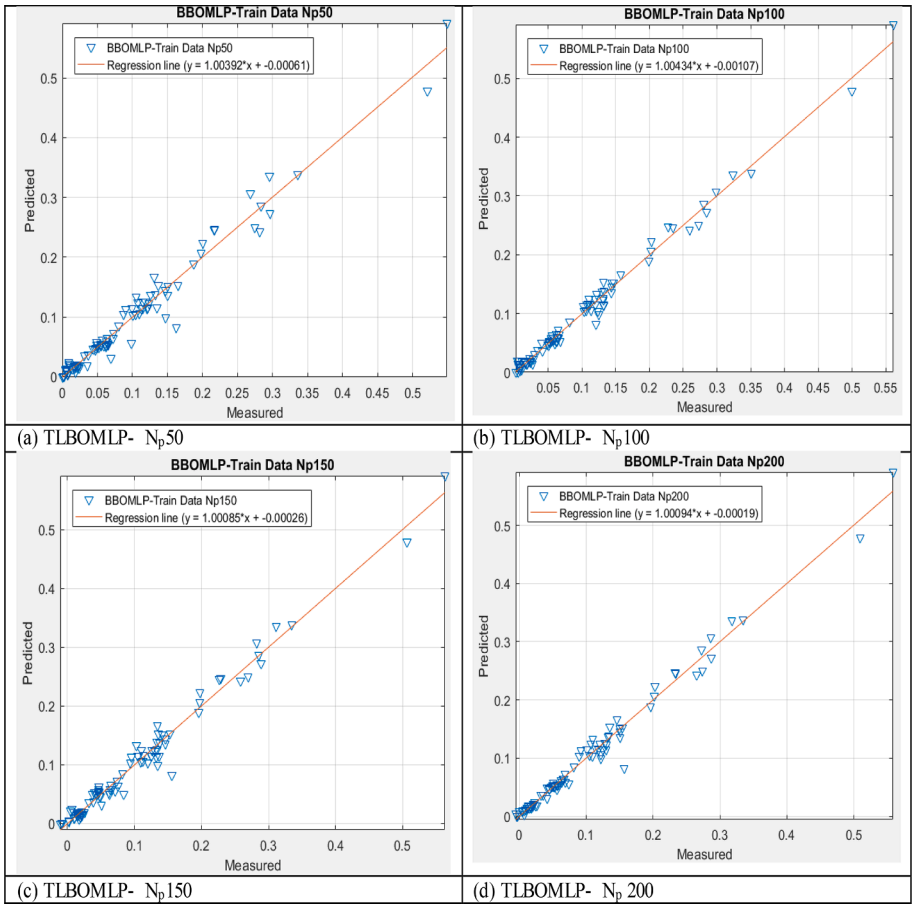

Fig. 8. Accuracy results of testing dataset for different proposed TLBOMLP structure.

[66]. TLBO models two basic phases of learning: (i) through the teacher and (ii) interacting with other learners [24]. A group of students (i.e., learners) is regarded as the population in the population-based algorithm known as TLBO, and the many topics presented to the learners are comparable to the various design parameters of the optimization issue. The learner's outcomes are equivalent to the issue's fitness value. It is generally agreed that the teacher offers the most effective solution out of the whole population. The TLBO algorithm's functioning is described below [65].

Teacher phase. This portion is essential for simulating the learning process between the teacher and the pupils (also referred to as learners). A teacher works to enhance the class's average score during this instruction phase by sharing knowledge with the pupils. Consider there is 'm' subjects (variables of design) offered to 'n' learners. At any ordinal teaching–learning cycle, *i*, $M_{i,j}$ is the mean result of the learners in a particular subject 'j' (j = 1, 2, …, m).

The best learner is regarded as a teacher in this algorithm because a teacher is the individual with the most expertise and understanding of a topic. Let $X_{total,kbest,i}$ represent the consequence of identifying the perfect learner as that cycle's teacher across all topics. To raise the knowledge's level, the teacher will exert her/his full commitment. However, students' levels of comprehension will be proportional to both the instruction's quality provided by the teacher and their fellow students' quality in the classroom. Because of this, the differential between the score of teacher's and the average student score for each topic is represented as follows:

$$\text{Difference\_Mean}_{j,i} = r_i(X_{j,kbest,i} - T_F M_{j,i}) \tag{4}$$

where $X_{j,kbest,i}$ indicates the teacher's result (i.e., best learner) in subject j. T_F represents the teaching factor, which determines the changed value of the mean, and r_i indicates a random number between [0 to 1]. The T_F value can be 1 or 2. The T_F is determined as follows:

$$T_F = \text{round}[1 + \text{rand}(0,1)\{2-1\}] \tag{5}$$

rand indicates a random number (between [0 to 1]). The T_F value is determined randomly by Eq. (5).

According to the following expression, based on the $\text{Difference}_{\text{Mean}_{j,i}}$, the current solution is updated in the teacher phase:

$$X'_{j,k,i} = X_{j,k,i} + \text{Difference\_Mean}_{j,i} \tag{6}$$

where $X'_{j,k,i}$ indicates the updated value of $X_{j,k,i}$ accept $X'_{j,k,i}$ if it gives a better function value. At the completion of the teacher phase, all approved function values are retained, and these values are the learner phase's input. The values of r_i and T_F influence the TLBO algorithm's performance. r_i is a random value from 0 to 1 and T_F represents the teaching factor. Nevertheless, the r_i and T_F values are obtained randomly, and these variables do not supply input. Therefore, the adjustment of r_i and T_F is not needed in the algorithm. For its operation, TLBO needs the adjustment of the general control variables, such as population size and frequency of generations. These variables are necessary for the process of all population-based algorithms. TLBO can be referred to as a parameter-less algorithm specific to an algorithm.

Learner phase. Student-to-student interaction is used to model the learning process in this algorithm phase, which models the students (or learners) learning. Discussions and interactions with other students can

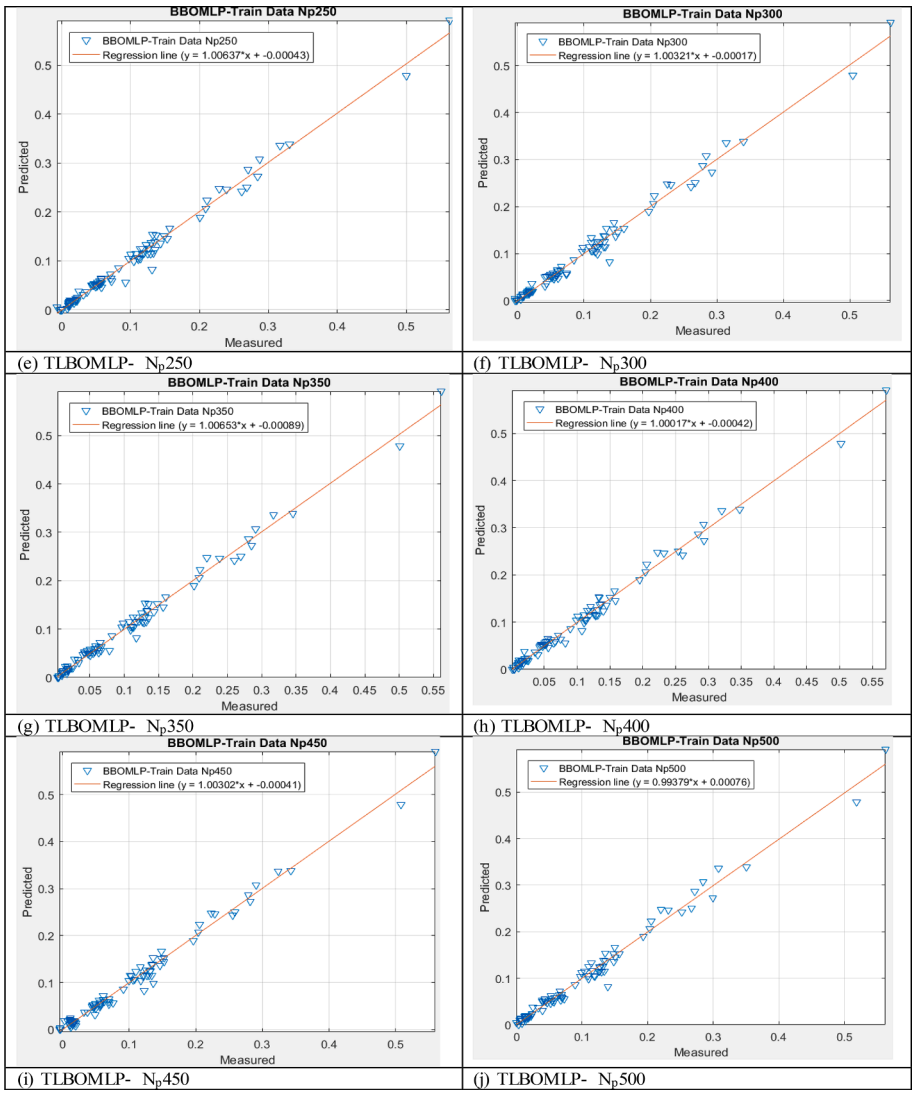

Fig. 8. (*continued*).

help them learn new things. When the other learners possess additional knowledge, then the learner will learn novel content. Following is an expression of the learning process that occurred during this phase. Randomly select two learners, *Q,* and *P,* such that $X'_{\text{total}-P,i} \neq X'_{\text{total}-Q,i}$, where, $X'_{\text{total}-P,i}$ and $X'_{\text{total}-Q,i}$ are the updated values of $X'_{\text{total}-P,i}$ and $X'_{\text{total}-Q,i}$, respectively, at the end of the teacher phase.

$$X''_{j,P,i} = X'_{j,P,i} + r_i\left(X'_{j,P,i} - X'_{j,Q,i}\right) if X'_{total-P,i} > X'_{total-Q,i} \tag{7}$$

$$X''_{j,P,i} = X'_{j,P,i} + r_i\left(X'_{j,Q,i} - X'_{j,P,i}\right) if X'_{total-Q,i} > X'_{total-P,i} \tag{8}$$

Accept $X''_{j,P,i}$ if it gives a better function value.

Results and discussion

The overall thermal transmission coefficient of the heat exchanger can be predicted using a conjunction of the ANN and two optimization approaches [67]. Randomly, the data are split into two groups, the training, and the testing set, each containing 80 % and 20 % of the total data. Each suggested optimizer is run for five hundred iterations, and ten different population sizes are evaluated. To complete the prediction, the appropriate population is selected. This population has the minimum RMSE and the largest quantity of R^2. Table 3 presents the R^2 and RMSE values for the BBO-MLP method under ten population sizes (50, 100, 150, 200, 250, 300, 350, 400, 450, and 500) for each training and testing data subset. These values are applicable to both sets of data. According to what can be shown, the population size of 500 yields the optimum results for the BBO-MLP approach. There are ten different population sizes; therefore, the score ranges from one to ten, with one being awarded to the population size with the highest score possible and ten being given to the population size with the lowest score possible. It is essential to highlight that R^2 ought to be higher, whereas RMSE needs to be lower for the ideal condition. In other terms, the lowest RMSE and highest R^2 values receive the highest score. Fig. 4 illustrates the value of the RMSE for each of the ten different population sizes.

As determined by the BBO method, Figs. 5 and 6 indicate a comparison of the anticipated and actual values of each population size. Training and testing stages have RMSE values of 0.01122 and 0.06112, respectively, for this model. Additionally, concerning the testing and the training phases, the R2 for BBO-MLP are 0.95175 and 0.9943, respectively.

Table 4 contains a tabulation of the R^2 and RMSE under ten population sizes for the TLBO-MLP instance. During the course of testing, the population sizes of 400 and 50 correspond to those with minimal and maximal errors. In conclusion, the population size of 400 is associated with the greatest performance in the training and the testing data specimens. Figs. 7 and 8, regarding the training and testing data

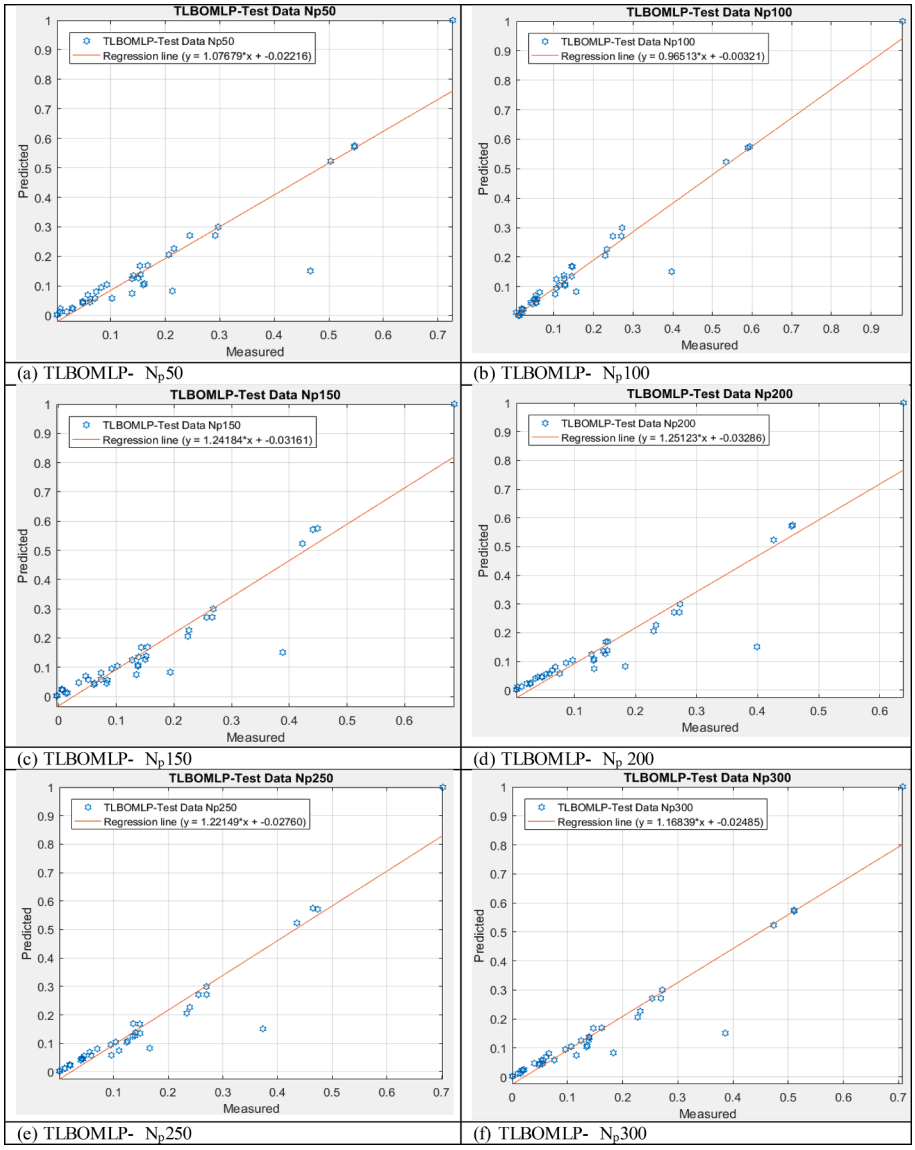

Fig. 9. The error and frequency of MAE for the best fit BBOMLP proposed model.

specimens, compare the modeled and predicted population size values for all population sizes.

Table 3 displays the RMSE and R^2 values for the BBO-MLP approach when applied to various population sizes. Accordingly, the population size of 500 has the minimum RMSE in training and testing procedures. When looking at the RSME and R^2 and in the train and test stages, this approach achieves its highest level of performance with a population size of 500. This is true regardless of the data set. Figures 13 and 14 present a graphical representation of the comparisons between the modeled and anticipated values.

Table 4 represents the RMSE and R2 values associated with the TLBO approach for both the training and testing sets. Among all population sizes, the 400-person population displays the maximum efficiency. Compared to the other techniques, the TLBO method achieves its highest performance with the smallest possible population size. In addition, when it came to forecasting the overall heat loss, the BBO algorithm is the one that performs the least well.

This section compares the outputs (the anticipated heat loss) with the target values (the measured heat loss) in order to appraise the performance of the BBO-MLP and TLBO-MLP models. Figs. 9 and 10 illustrate the results of the training and testing datasets and the difference between each set of heat loss (output and target). For the training data samples, BBO-MLP and TLBO-MLP have MAE values of (0.0076668 and 0.007674), and RMSE values of (0.00012732 and 0.010132), and the testing data samples have the MAE values of (0.03232 and 0.026233), and RMSE values of (0.0045911 and 0.056967), respectively. For the training phase, the acquired error values are within the range of [-0.0006078, 0.01133] and [-0.00040708, 0.010181] for the predictions of the BBO-MLP and TLBO-ANFIS for the best fit, respectively. Also, the testing errors are within the [0.0004724, 0.068666] and [0.0021984, 0.057688] range for the BBO-MLP and TLBO-MLP methods, respectively. The TLBO-MLP's lowest amount of errors demonstrates how well this model predicts heat loss. Before this, other studies have been conducted in this field, and more studies are needed to be able to suggest the use of ANN methods in predicting heat loss. To increase the precision of calculating the heat loss of buildings and

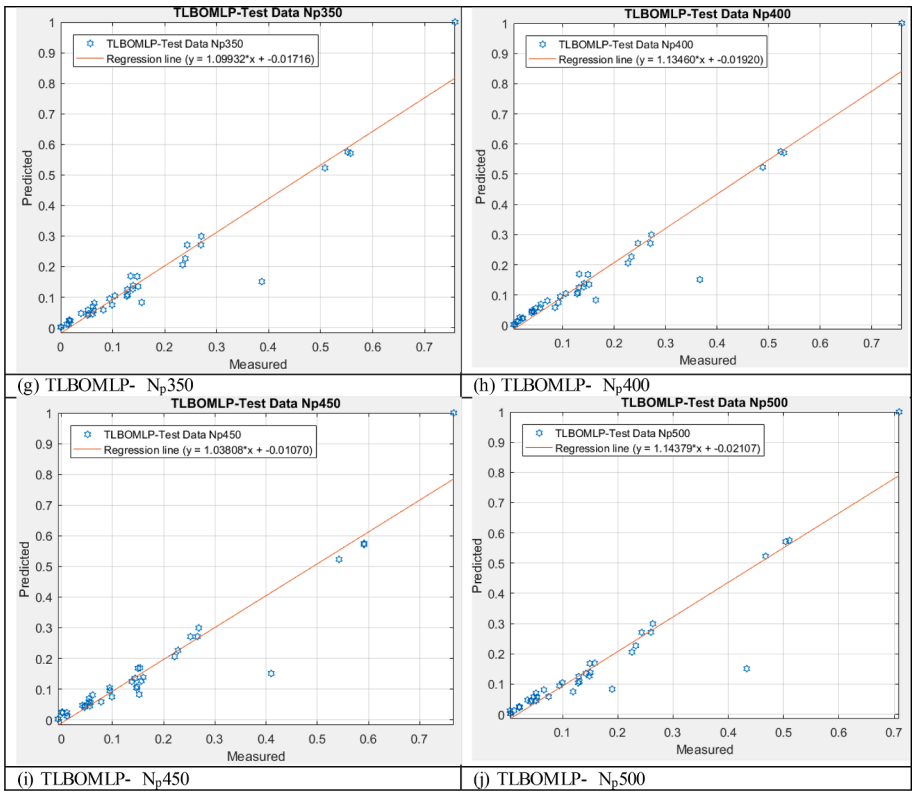

Fig. 9. (*continued*).

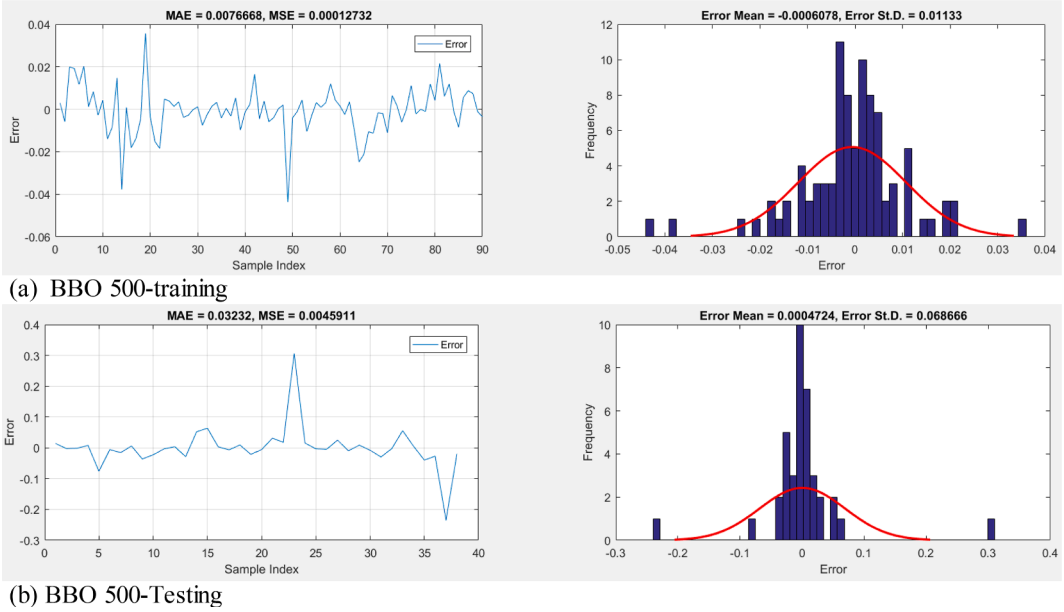

Fig. 10. The error and frequency of MAE for the best fit TLBOMLP proposed model.

explicitly integrating them with optimization algorithms, further study is required. Table 5 indicates the previous research in the energy field.

Conclusions

In order to optimize a building's energy efficiency and achieve energy conservation and environmental impact reduction, it is important to forecast how much energy it will need. This study uses a mathematical simulation to determine the overall thermal transmission (heat loss) and create a database for ANN application. The MLP neural network was integrated with two hybrid algorithms (BBO and TLBO) to reduce errors and improve ANN performance. An agent (i.e., a technique with a lower RMSE, higher R2, and lower MAE) is chosen for each optimizer technique, separated into ten populations. To determine which approach is the most accurate, several agents of techniques were ultimately compared to one another. The TLBO provides superior outcomes in this particular scenario among the two methods due to its low error values and higher R^2 values. The population size of 400 provides the optimal

Table 5
Heat loss field researches.

Number	Paper name	Authors	References
1	A new ANN-based technique to evaluate the heat transfer coefficients in the heating systems in wall	Acikgoz, Çebi, Dalkilic, Koca, Çetin, Gemici, Wongwises	[68]
2	Use ANN to forecast the overall heat transfer coefficient on a simulated heat exchanger	Reynoso-Jardón, Tlatelpa-Becerro, Rico-Martínez, Calderón-Ramírez, Urquiza	[69]
3	Performance of ANN in forecasting the Heat Transfer through Walls subjected to fire	Bakas, Kontoleon	[70]
4	Evaluation of the heat loss coefficient of two residential buildings via an average method	Uriarte, Erkoreka, Eguia, Granada, Martin-Escudero	[40]
5	Heat loss coefficient evaluation applied to buildings via machine learning (ML) models	Martínez-Comesaña, Febrero-Garrido, Granada-Álvarez, Martínez-Torres, Martínez-Mariño	[71]
6	Wall and insulation materials' application in green building	Wang, Chiang, Cai, Li, Wang, Chen, Wei, Huang	[72]
7	Reducing heat loss in buildings through Renewable materials: date palm wood's Characterization	Agoudjil, Benchabane, Boudenne, Ibos, Fois	[73]

performance for the TLBO. The suggested model's output is calculated using RMSE of 0.01012 and 0.05216 in the training and testing phases. The BBO algorithm is the approach that was less accurate for calculating the overall thermal transmission coefficient. It exhibits an RMSE of 0.01122 for the training data and 0.06112 for the testing data. Also, according to the training error ranges of [-0.0006078, 0.01133] and [-0.00040708, 0.010181] and testing error ranges of [0.0004724, 0.068666] and [0.0021984, 0.057688] for BBO-MLP and TLBO-MLP, respectively, shows that the TLBO-MLP reaches the lower range of error and can predict the heat loss with higher accuracy.

CRediT authorship contribution statement

Hossein Moayedi: Conceptualization, Methodology, Formal analysis, Investigation, Writing - Original Draft, Writing - Review & Editing, Funding acquisition. **Hasan Yildihzan:** Funding acquisition, Writing - Review & Editing, Supervision. **Pasura Aungkulanon:** Writing - Review & Editing. **Yulineth Cardenas Escorcia:** Validation, Visualization, Writing - Original Draft. **Mohammed Al-Bahrani:** Writing - Review & Editing. **Binh Nguyen Le:** Methodology.

Declaration of Competing Interest

The authors declare that they have no known competing financial interests or personal relationships that could have appeared to influence the work reported in this paper.

Data availability

No data was used for the research described in the article.

References

[1] CHANGE, I.P.O.C., Report of the Nineteenth Session of the Intergovernmental Panel on Climate Change *(IPCC) Geneva, 17-20 (am only) April 2002.* 2007.

[2] Yan B, et al. Geometrically enabled soft electroactuators via laser cutting. Adv Eng Mater 2019;21(11):1900664.

[3] Heydari A, Sadati SE, Gharib MR. Effects of different window configurations on energy consumption in building: optimization and economic analysis. J Build Eng 2021;35:102099.

[4] de Gastines M, Correa É, Pattini A. Heat transfer through window frames in EnergyPlus: model evaluation and improvement. Adv Build Energy Res 2019;13 (1):138–55.

[5] Al-Ghaili AM, et al. Energy management systems and strategies in buildings sector: A scoping review. IEEE Access 2021;9:63790–813.

[6] Agency EE. Final energy consumption by sector and fuel. Belgium: European Environment Agency Brussels; 2015.

[7] Ahmadi-Karvigh S, et al. Real-time activity recognition for energy efficiency in buildings. Appl Energy 2018;211:146–60.

[8] Sadeghian O, et al. A comprehensive review on energy saving options and saving potential in low voltage electricity distribution networks: Building and public lighting. Sustain Cities Soc 2021;72:103064.

[9] Huang Y, Li C. Accurate heating, ventilation and air conditioning system load prediction for residential buildings using improved ant colony optimization and wavelet neural network. Journal of Building Engineering 2021;35:101972.

[10] Sarihi S, Saradj FM, Faizi M. A critical review of façade retrofit measures for minimizing heating and cooling demand in existing buildings. Sustain Cities Soc 2021;64:102525.

[11] Chen Y, et al. Life cycle assessment of greenhouse gas emissions and water-energy optimization for shale gas supply chain planning based on multi-level approach: Case study in Barnett, Marcellus, Fayetteville, and Haynesville shales. Energ Conver Manage 2017;134:382–98.

[12] Adnan Ikram RM, Ewees AA, Parmar KS, Yaseen ZM, Shahid S, Kisi O. The viability of extended marine predators algorithm-based artificial neural networks for streamflow prediction. Applied Soft Computing 2022;131:109739. https://doi.org/10.1016/j.asoc.2022.109739.

[13] Hewawasam V, Matsui K. Historical development of climate change policies and the Climate Change Secretariat in Sri Lanka. Environ Sci Policy 2019;101:255–61.

[14] Ascione F, et al. Building envelope design: multi-objective optimization to minimize energy consumption, global cost and thermal discomfort. Application to different Italian climatic zones. Energy 2019;174:359–74.

[15] Echenagucia TM, et al. The early design stage of a building envelope: multi-objective search through heating, cooling and lighting energy performance analysis. Appl Energy 2015;154:577–91.

[16] Ciulla G, et al. Application of optimized artificial intelligence algorithm to evaluate the heating energy demand of non-residential buildings at European level. Energy 2019;176:380–91.

[17] Wu W, et al. A multi-objective optimization design method in zero energy building study: A case study concerning small mass buildings in cold district of China. Energy Build 2018;158:1613–24.

[18] Li H, Wang S, Cheung H. Sensitivity analysis of design parameters and optimal design for zero/low energy buildings in subtropical regions. Appl Energy 2018; 228:1280–91.

[19] Wu P, et al. Autonomous surface crack identification of concrete structures based on an improved one-stage object detection algorithm. Eng Struct 2022;272: 114962.

[20] Alnaqi AA, et al. Prediction of energetic performance of a building integrated photovoltaic/thermal system thorough artificial neural network and hybrid particle swarm optimization models. Energ Conver Manage 2019;183:137–48.

[21] Zhao Y, et al. Fragility analyses of bridge structures using the logarithmic piecewise function-based probabilistic seismic demand model. Sustainability 2021;13(14): 7814.

[22] Muhammad S, et al. Sustainable green information systems design: a theoretical model. Acta Informatica Malaysia 2017;1(2):3–4.

[23] Nebot À, Mugica F. Energy performance forecasting of residential buildings using fuzzy approaches. Appl Sci 2020;10(2):720.

[24] Almutairi K, et al. A TLBO-Tuned Neural Processor for Predicting Heating Load in Residential Buildings. Sustainability 2022;14(10):5924.

[25] Xie X, Sun Y. A piecewise probabilistic harmonic power flow approach in unbalanced residential distribution systems. Int J Electr Power Energy Syst 2022; 141:108114.

[26] Nguyen H, et al. Proposing a novel predictive technique using M5Rules-PSO model estimating cooling load in energy-efficient building system. Eng Comput 2020;36 (3):857–66.

[27] Guo Z, et al. Optimal modification of heating, ventilation, and air conditioning system performances in residential buildings using the integration of metaheuristic optimization and neural computing. Energy Build 2020;214:109866.

[28] Wang R, Lu S, Feng W. A novel improved model for building energy consumption prediction based on model integration. Appl Energy 2020;262:114561.

[29] Abd Alla S, et al. Life-cycle approach to the estimation of energy efficiency measures in the buildings sector. Appl Energy 2020;264:114745.

[30] Sadeghi A, et al. An intelligent model to predict energy performances of residential buildings based on deep neural networks. Energies 2020;13(3):571.

[31] Metallidou CK, Psannis KE, Egyptiadou EA. Energy efficiency in smart buildings: IoT approaches. IEEE Access 2020;8:63679–99.

[32] Bui X-N, Moayedi H, Rashid ASA. Developing a predictive method based on optimized M5Rules–GA predicting heating load of an energy-efficient building system. Eng Comput 2020;36(3):931–40.

[33] Luo X, et al. Comparative study of machine learning-based multi-objective prediction framework for multiple building energy loads. Sustain Cities Soc 2020; 61:102283.

[34] Foong LK, et al. Efficient metaheuristic-retrofitted techniques for concrete slump simulation. Smart Struct Syst Int J 2021;27(5):745–59.
[35] Zhao Y, et al. Deterministic snap-through buckling and energy trapping in axially-loaded notched strips for compliant building blocks. Smart Mater Struct 2020;29 (2):p. 02LT03.
[36] Wang Z, Hong T, Piette MA. Building thermal load prediction through shallow machine learning and deep learning. Appl Energy 2020;263:114683.
[37] Adnan Ikram RM, Dai H-L, Ewees AA, Shiri J, Kisi O, Zounemat-Kermani M. Application of improved version of multi verse optimizer algorithm for modeling solar radiation. Energy Reports 2022;8:12063–80. https://doi.org/10.1016/j.egyr.2022.09.015.
[38] Ozarisoy B. Energy effectiveness of passive cooling design strategies to reduce the impact of long-term heatwaves on occupants' thermal comfort in Europe: climate change and mitigation. J Clean Prod 2022;330:129675.
[39] Yu D, et al. Optimal performance of hybrid energy system in the presence of electrical and heat storage systems under uncertainties using stochastic p-robust optimization technique. Sustain Cities Soc 2022;83:103935.
[40] Uriarte I, et al. Estimation of the heat loss coefficient of two occupied residential buildings through an average method. Energies 2020;13(21):5724.
[41] Naphon P, et al. ANN, numerical and experimental analysis on the jet impingement nanofluids flow and heat transfer characteristics in the micro-channel heat sink. Int J Heat Mass Transf 2019;131:329–40.
[42] Gao W, et al. Comprehensive preference learning and feature validity for designing energy-efficient residential buildings using machine learning paradigms. Appl Soft Comput 2019;84:105748.
[43] Moya-Rico J, et al. Characterization of a triple concentric-tube heat exchanger with corrugated tubes using Artificial Neural Networks (ANN). Appl Therm Eng 2019; 147:1036–46.
[44] Zhou G, Moayedi H, Foong LK. Teaching–learning-based metaheuristic scheme for modifying neural computing in appraising energy performance of building. Eng Comput 2021;37(4):3037–48.
[45] Ren Z, Motlagh O, Chen D. A correlation-based model for building ground-coupled heat loss calculation using Artificial Neural Network techniques. J Build Perform Simul 2020;13(1):48–58.
[46] Abiodun OI, et al. State-of-the-art in artificial neural network applications: A survey. Heliyon 2018;4(11):e00938.
[47] Wang, S.-C., *Artificial Neural Network*, in *Interdisciplinary Computing in Java Programming*, S.-C. Wang, Editor. 2003, Springer US: Boston, MA. p. 81-100.
[48] Zhao Y, Foong LK. Predicting electrical power output of combined cycle power plants using a novel artificial neural network optimized by electrostatic discharge algorithm. Measurement 2022:111405.
[49] Zhao Y, et al. Predicting compressive strength of manufactured-sand concrete using conventional and metaheuristic-tuned artificial neural network. Measurement 2022;194:110993.
[50] Liu L, et al. Optimizing an ANN model with genetic algorithm (GA) predicting load-settlement behaviours of eco-friendly raft-pile foundation (ERP) system. Eng Comput 2020;36(1):421–33.
[51] Zhao Y, et al. A novel artificial bee colony algorithm for structural damage detection. Adv Civ Eng 2020;2020.
[52] Feindt M, Kerzel U. The NeuroBayes neural network package. Nucl Instrum Methods Phys Res, Sect A 2006;559(1):190–4.
[53] Zhao Y, Wang Z. Subset simulation with adaptable intermediate failure probability for robust reliability analysis: an unsupervised learning-based approach. Struct Multidiscip Optim 2022;65(6):1–22.
[54] Moayedi H, et al. Applicability and comparison of four nature-inspired hybrid techniques in predicting driven piles' friction capacity. Transp Geotech 2022: 100875.
[55] Hecht-Nielsen, R., *III.3 - Theory of the Backpropagation Neural Network**Based on "nonindent" by Robert Hecht-Nielsen, which appeared in Proceedings of the International Joint Conference on Neural Networks 1, 593–611, June 1989. © 1989 IEEE*, in *Neural Networks for Perception*, H. Wechsler, Editor. 1992, Academic Press. p. 65-93.
[56] Yilmaz I. Landslide susceptibility mapping using frequency ratio, logistic regression, artificial neural networks and their comparison: a case study from Kat landslides (Tokat—Turkey). Comput Geosci 2009;35(6):1125–38.
[57] Prakash N, Manconi A, Loew S. A new strategy to map landslides with a generalized convolutional neural network. Sci Rep 2021;11(1):9722.
[58] Moayedi H, et al. Two novel neural-evolutionary predictive techniques of dragonfly algorithm (DA) and biogeography-based optimization (BBO) for landslide susceptibility analysis. Geomat Nat Haz Risk 2019;10(1):2429–53.
[59] Wilson, E.O. and R.H. MacArthur, *The theory of island biogeography*. Vol. 1. 1967: JSTOR.
[60] Simon D. Biogeography-based optimization. IEEE Trans Evol Comput 2008;12(6): 702–13.
[61] Ma H. An analysis of the equilibrium of migration models for biogeography-based optimization. Inf Sci 2010;180(18):3444–64.
[62] Ma H, Simon D. Blended biogeography-based optimization for constrained optimization. Eng Appl Artif Intel 2011;24(3):517–25.
[63] Rao RV, Savsani VJ, Vakharia D. Teaching–learning-based optimization: a novel method for constrained mechanical design optimization problems. Comput Aided Des 2011;43(3):303–15.
[64] Rao RV, Savsani VJ, Vakharia D. Teaching–learning-based optimization: an optimization method for continuous non-linear large scale problems. Inf Sci 2012; 183(1):1–15.
[65] Rao R, Patel V. An elitist teaching-learning-based optimization algorithm for solving complex constrained optimization problems. Int J Ind Eng Comput 2012;3 (4):535–60.
[66] Zhao Y, et al. Employing TLBO and SCE for optimal prediction of the compressive strength of concrete. Smart Struct Syst 2020;26(6):753–63.
[67] Zhao Y, Zhong X, Foong LK. Predicting the splitting tensile strength of concrete using an equilibrium optimization model. Steel Compos Struct Int J 2021;39(1): 81–93.
[68] Acikgoz O, et al. A novel ANN-based approach to estimate heat transfer coefficients in radiant wall heating systems. Energy Build 2017;144:401–15.
[69] Reynoso-Jardón E, et al. Artificial neural networks (ANN) to predict overall heat transfer coefficient and pressure drop on a simulated heat exchanger. Int J Appl Eng Res 2019;14(13):3097–103.
[70] Bakas I, Kontoleon KJ. Performance Evaluation of Artificial Neural Networks (ANN) Predicting Heat Transfer through Masonry Walls Exposed to Fire. Appl Sci 2021;11(23):11435.
[71] Martínez-Comesaña M, et al. Heat loss coefficient estimation applied to existing buildings through machine learning models. Appl Sci 2020;10(24):8968.
[72] Wang H, et al. Application of wall and insulation materials on green building: a review. Sustainability 2018;10(9):3331.
[73] Agoudjil B, et al. Renewable materials to reduce building heat loss: Characterization of date palm wood. Energy Build 2011;43(2–3):491–7.